SUPPLEMENTARY INFORMATION

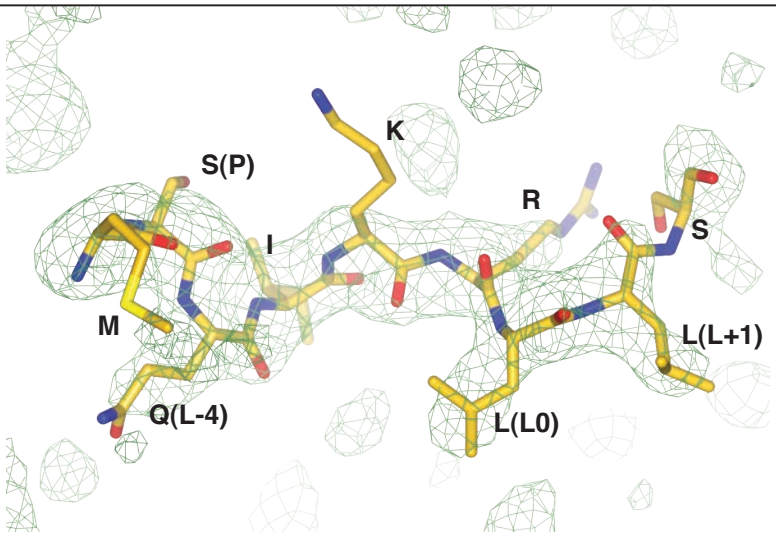

Figure S1a

Difference electron density (mFo - DFc) for the peptide (Q-peptide), from the first round of refinement after molecular replacement before building the peptide into the model. Contour level 0.08 e/Å^3. The electron density is clear for the two leucine residues and the main chain, but less so for the glutamine (-4) side chain. This and all other structure figures were made using CCP4mg (Potterton, L. et al. Developments in the CCP4 molecular-graphics project. *Acta Crystallogr D Biol Crystallogr* **60**, 2288-94 (2004)).

R	M	Sp	Q	I	K	R	L	L	S	E
-7	**-6**	**-5**	**-4**	**-3**	**-2**	**-1**	**0**	**+1**	**+2**	**+3**

Figure S1b

Sequence of the Q-peptide with the numbering scheme relative to the first leucine as 0. The "E-peptide" has Q(L-4) replaced by E

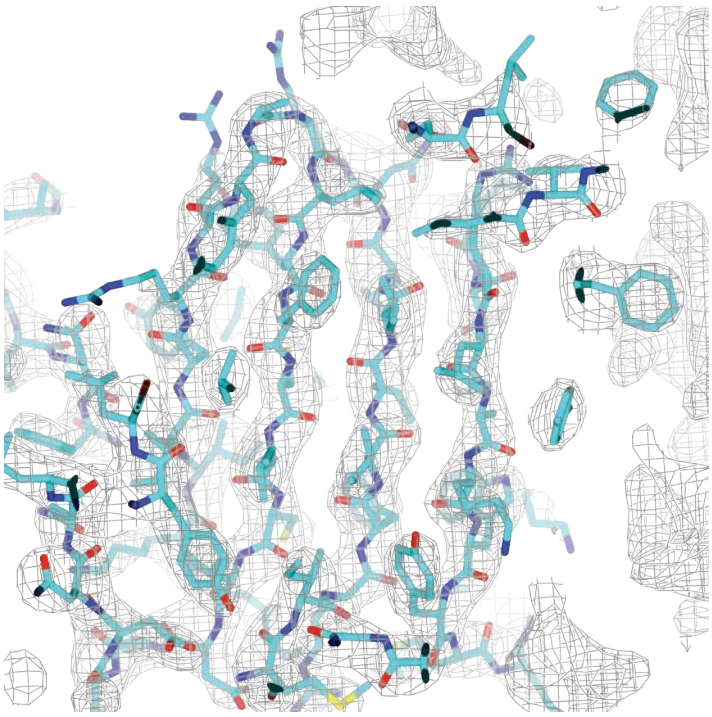

Figure S2

A sample of the final refined 2mFo - DFc electron density map for the Q-peptide structure, through the β-sheet in the σ2 subunit, contoured at 0.18 e/Å^3

Dataset	**Q peptide**	**E peptide**
Space group, unit cell (a, c)	$P4_32_12$, 169.9, 321.7 Å	$P4_32_12$, 171.2,324.3 Å
Wavelength	0.976 Å	0.976 Å
Rotation range (nearest axis to spindle)	112° (c*)	114° (a*)
Resolution range Å (high resolution)	51–3.0 (3.16-3.0)	47-3.4 (3.58-3.40)
R_{merge}	0.198 (1.17)	0.195 (0.96)
R_{merge} in top intensity bin	0.050	0.058
R_{meas}	0.223 (1.32)	0.212 (1.06)
R_{pim}	0.102	0.079 (0.42)
Number of observations (unique)	853264 (96683)	410234 (64153)
$< <I_h> / \sigma(<I_h>) >$	8.6 (1.8)	7.8 (1.9)
Completeness	100.0% (100.0%)	95.8% (89.1%)
Multiplicity	8.8 (9.0)	6.4 (5.0)
Wilson <B>	60Å^2	58 Å^2
Refinement		
R_{work}	0.204 (0.33)	0.24 (0.33)
R_{free}	0.261 (0.37)	0.267 (0.38))
Number of reflections (test set)	183747 (9168)	116095 (5902)
RMSD bonds (angles)	0.007Å (1.1°)	0.009Å (1.3°)
Number of TLS groups	28	28
$<B_{iso}>$ (peptides)	79Å^2 (84Å^2)	86Å^2 (108Å^2)
Number of atoms	28125	28125
Number of sulphate ions (waters)	34 (26)	34 (26)

Supplementary Table S1: Data collection & refinement statistics.

$R_{merge} = \Sigma_{hl} | I_{hl} - <I_h> | / \Sigma_{hl} <I_h>$; $R_{meas} = \Sigma_{hl} [n_h/(n_h-1)]^{1/2} I_{hl} - <I_h> | / \Sigma_{hl} <I_h>$

$R_{pim} = \Sigma_{hl} [1/(n_h-1)]^{1/2} I_{hl} - <I_h> | / \Sigma_{hl} <I_h>$ where n_h is the number of observations of reflection **h**.

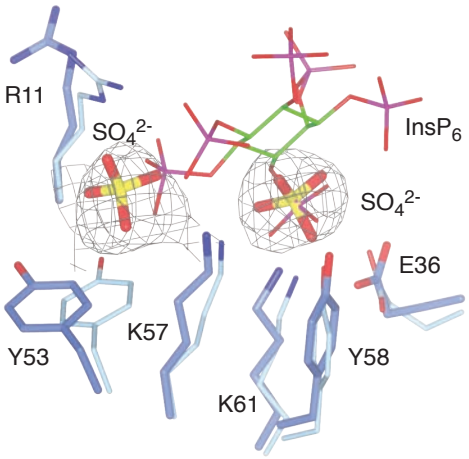

Figure S3

Refined electron density for the two sulphate ions (contoured at 0.18 e/Å^3, cropped around the sulphates) which bind to the α subunit, mimicking the binding of $InsP_6$ seen in the inactive structure (thin bonds). All labelled side chains are in the α subunit.

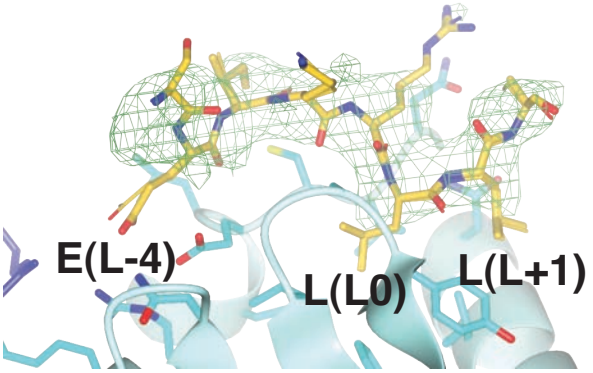

Figure S4

Difference electron density (mFo - DFc) for the "E-peptide" from the first round of refinement after molecular replacement before building the peptide into the model, contoured at 0.06 e/Å^3. The structure of the Q-peptide is shown with thin bonds.

	dileucine signal binding (tested for CD4 and LRP9)
wt core	+++
σ2V88D	-
σ2V98S	-
σ2V98F	+
σ2L103S	-
σ2A63W	-
σ2N92W	-
σ2L65S	++
σ2Y62S	-
σ2E100Y	-
σ2R15S/αR21E	+
σ2R15S/αR21S	+

Supplementary Table S2. : Binding of AP2 core mutants to dileucine sorting signals. The indicated AP2 core mutants were tested for binding to the dileucine signals of CD4 and LRP9 using the biosensor-based membrane mimic assay. ++ +: level of binding displayed by wt core, ++: affinity reduced by less than 5-fold; +: 5-10-fold reduced affinity; -: no detectable binding. We did not observe any obvious difference in binding to the dileucine signals of CD4 and LRP9, except that binding to the latter was generally slightly stronger (see table S3 for details).

Membrane protein	-5 -4 -3 -2 -1 L +1	Affinity for wt AP2 core (μM)
phospho-CD4 Q-peptide	ⓅSQIKRLL	0.85
phospho-CD4 E-peptide	ⓅSEIKRLL	0.65
Tyrosinase	EEKQPLL	0.6
TRP1	EANQPLL	0.75
Limp-II	DERAPLI	0.9
LRP9	AEDEPLL	0.55

Supplementary Table S3. Binding of AP2 core to a range of different dileucine signals.
Binding of AP2 cores to a number of different 'acidic dileucine' motifs displayed in PtdIns4,5P_2 containing liposomes was recorded in the biosensor-based membrane mimic assay and the rate constants were determined as described. Irrespective of the type of dileucine signal analysed, the K_{DS} for binding were in the range of 0.55 - 0.90 μM. Binding experiments to liposomes containing control peptides with mutated dileucine signals (LL replaced by AA) served as negative controls except in the case of LimpII where no peptide was available) showed that there was no binding to acidic dileucine motifs if the L[LI] group is replaced by AA (data not shown). This agrees with *in vivo* studies (Letourneur, F. & Klausner, R. D. A novel di-leucine motif and a tyrosine-based motif independently mediate lysosomal targeting and endocytosis of CD3 chains. *Cell* **69**, 1143-57 (1992)) and our unpublished data showing that a reporter construct consisting of the lumenal and transmembrane regions of CD8 fused to the cytosolic signal of LRP (cytosolic sequence SHAGSRATEASEDEPLLSS) was endocytosed from the plasma membrane whereas replacing LL with AA prevented uptake of a reporter construct without affecting YxxΦ-based endocytosis of transferrin (data not shown).

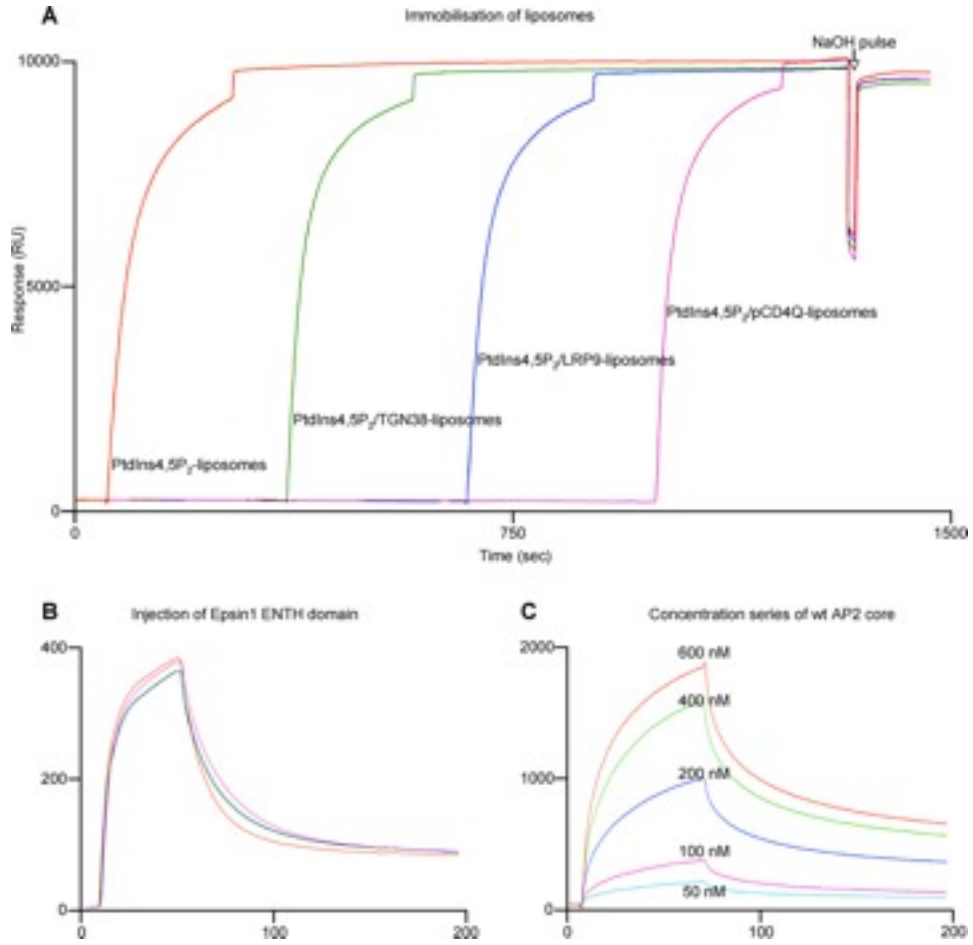

Figure S5 Liposome capture and analysis.

a : Sequential injection of the indicated types of liposomes on the 4 flow-cells of a BIAcore L1 sensor surface. After capture all flow-cells were treated with NaOH to generate a stable surface for further injections. **b**: After liposome capture as in a, the ENTH-domain of epsin1 was passed over all 4 flow-cells to reveal the amount of PtdIns4,5P_2 in the different liposomes. Note that the peak of the sensorgrams differ by less than 20RU demonstrating equal amounts of PtdIns4,5P_2 in the 4 different liposome preparations. **c**: Superimposition of sensorgrams obtained for the binding of varying concentrations of the wt AP2 core to the phosphorylated CD4-Q peptide. The plots were further used to calculate the rate constants and K_D of the interaction and similar plots were used to derive all K_D values mentioned throughout the manuscript.

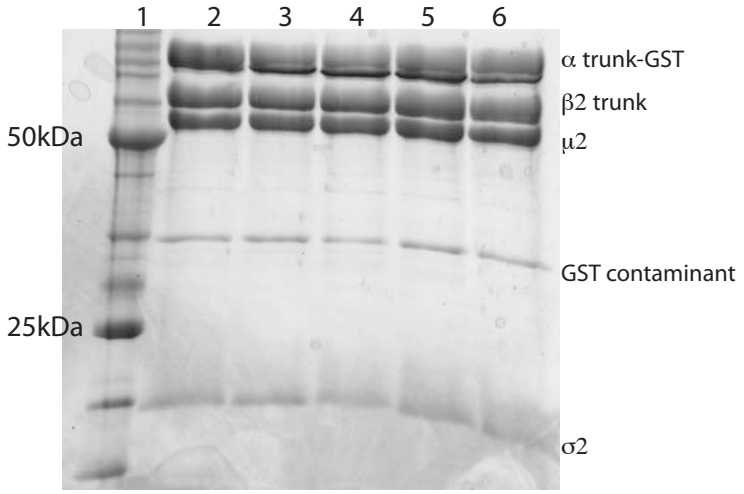

Figure S6

Coomassie brilliant blue stained SDS PAGE Gel showing GST core proteins used for K_D determinations shown in Figure3. *Lane1* Molecular weight markers, *lane2* wt AP2 core, *lane3* σ2V88D, *lane4* σ2 L103S, *lane5* σ2R15S/ αR21S *lane6* σ2R15S/αR21E

Figure S7

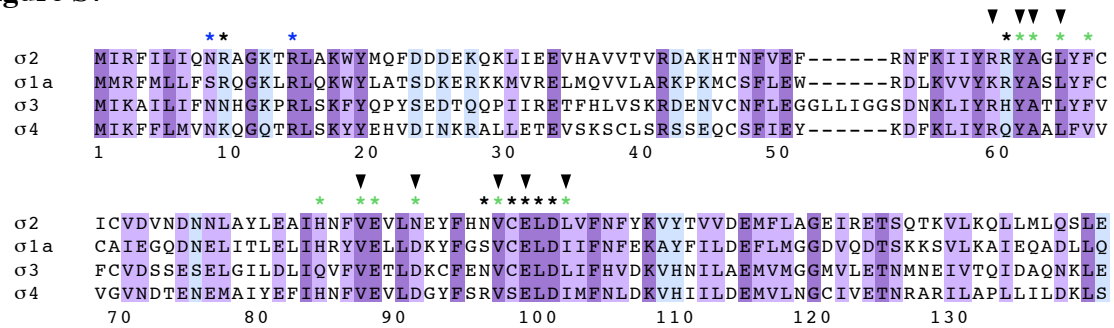

a The residues involved in binding the acidic and dihydrophobic parts of acidic dileucine motifs are conserved in all σ subunits from mammalian AP complexes. Mammalian σ2 (1-142), σ1a (1-124), σ3 (1-148) and σ4 (1-142) were aligned using ClustalW. The resulting output was coloured as follows: deep purple indicates absolute conservation, purple indicates a high degree of conservation and light purple indicates a modest degree of conservation. The results have been plotted on surface representations of σ2 in the Q peptide complex in figure 2. σ2 residues are numbered beneath the alignment. Coloured asterisks indicate residues involved in binding to the CD4 peptide; blue asterisks mark residues involved in binding to the -4 position peptide residue (Q in this case); green asterisks mark residues involved in binding the LL motif and black asterisks indicate residues contacting other parts of the peptide. Mutations in residues marked with a black arrow abrogate or greatly diminish binding to dileucine peptides.

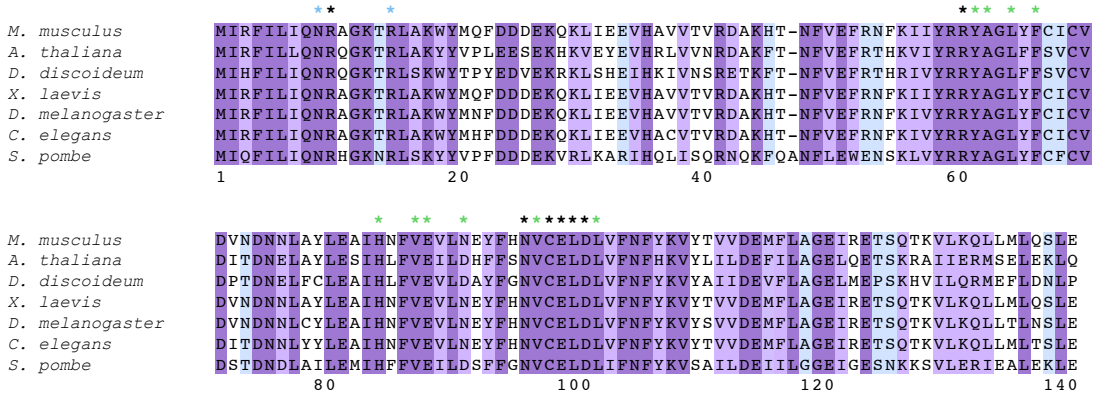

b The residues involved in binding the acidic and dihydrophobic parts of acidic dileucine motifs are conserved in σ2 subunits from a variety of species from yeast to mammals. σ2 (residues 1-142) proteins from various species were aligned using ClustalW and the resulting output coloured and annotated as in **a**. *M. musculus* σ2 residues are numbered beneath the alignment.

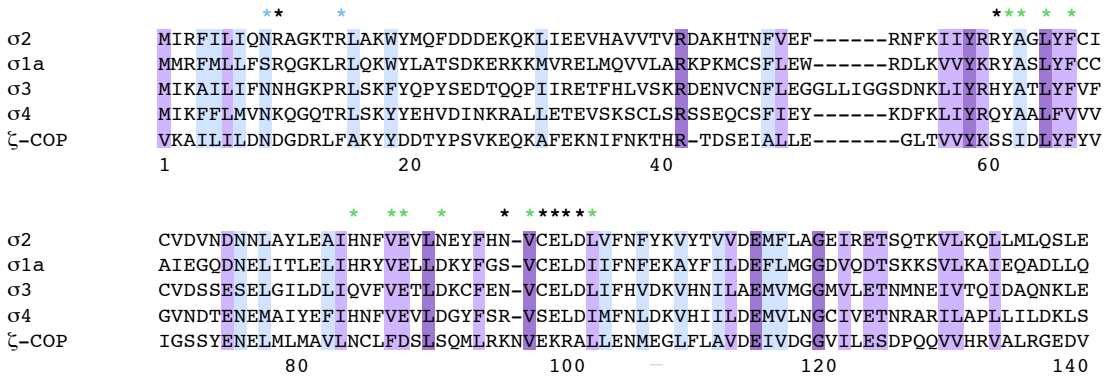

c The residues involved in binding only the dihydrophobic part of the acidic dileucine motif are conserved between mammalian σ subunits and the homologous ζCOP. The sequences of mammalian σ2 (1-142), σ1a (1-124), σ3 (1-148) and σ4 (1-142) and ζCOP (13-153) (PDB id 2HF6) were aligned using ClustalW and the resulting output coloured and annotated as in **a**.

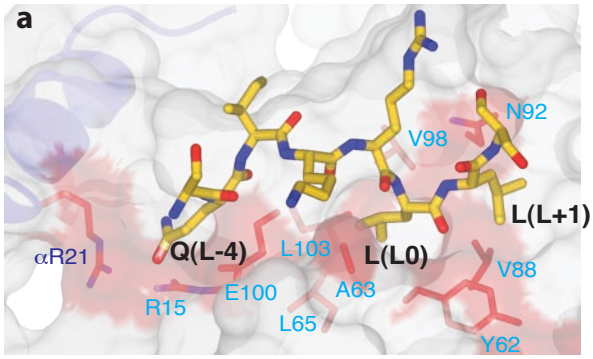

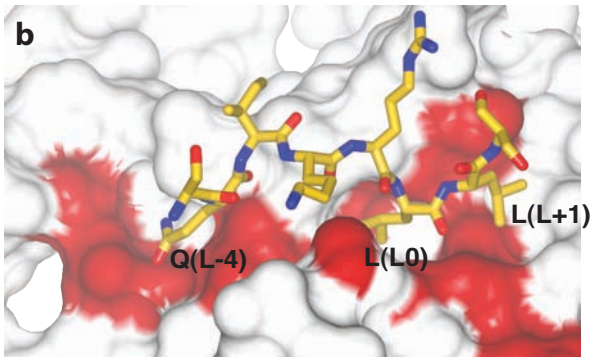

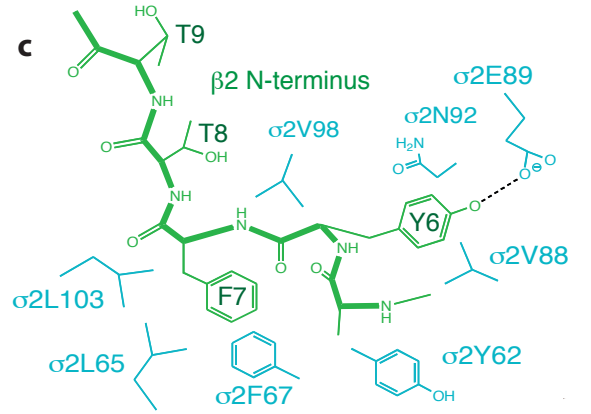

Figure S8

a Structure of the dileucine peptide binding site showing the peptide in gold. Residues coloured red are those whose mutation strongly inhibits dileucine peptide binding whilst not affecting YxxΦ motif binding (See table S3). Labels for mutated residues are coloured pale blue for σ2 and dark blue for α. The protein is displayed as a semi-transparent surface coloured red where underlying mutations effect dileucine peptide binding.

b The same as **a** with the surface drawn solid.

c Schematic diagram of the contacts made by the β2 N-terminus to the LL peptide site on σ2 in the inactive IP_6-liganded structure. The hydrophobic residues Y6 and F7 occupy equivalent sites to the two leucines L+1 and L0 in the peptide, with the main chain running in the opposite direction (compare with figures 2b and 4c). Other interactions are not conserved.

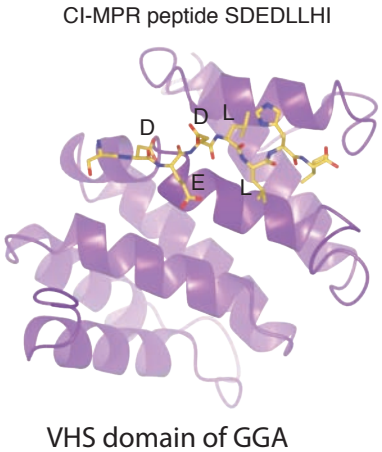

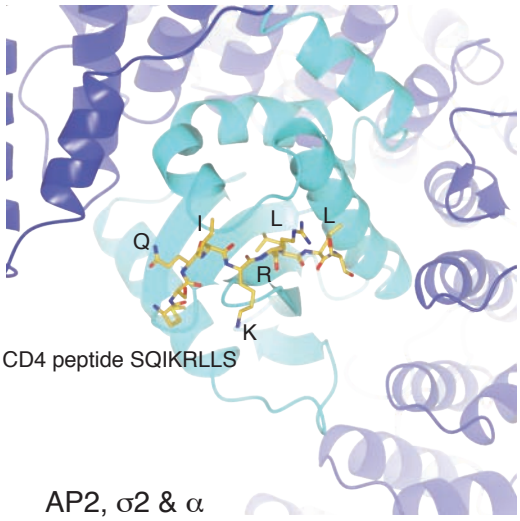

Figure S9

The mechanisms of binding of [ED]xxxL[LI] to σ2/α of AP2 and of DxxLL to the GGA VHS domain are completely different, and are based on different underlying structures. a DxxLL motif in gold binding to the GGA VHS domain (purple) **b** [ED]xxxL[LI] motif shown in gold binding to σ2(pale blue) and α(dark blue). The peptides are shown in approximately the same orientation